Journal of Physical Chemistry and Functional Materials

Home Page of Journal: https://dergipark.org.tr/jphcfum

Quantum Chemical Calculation Employed for Investigation Mesitylene Compound

Rebaz Obaid Kareem [a], Othman Abdulrahman Hamad [b], Rebaz Anwar Omer [c], Yousif Hussein Azeez[a], Lana Omer Ahmed[d], Khdir Ahmed Othman[c], Omer Kaygili [e]

[a]*Physics Department, College of Science, University of Halabja, 46018, Halabja, Iraq*
[b]*University of Raparin, College of Science, Department of Chemistry, Sulamani, Iraq*
[c]*Koya University, Faculty of Science & Health, Department of Chemistry, Koya KOY45, Kurdistan Region – F.R., Iraq*
[d]*Koya University, Faculty of Science & Health, Department of Physics, Koya KOY45, Kurdistan Region – F.R., Iraq*
[e]Department of Physics, Faculty of Science, Firat University, 23119, Elazig, Türkiye
* Corresponding author: E-mail: obedrebaz9@gmail.com

ABSTRACT

The purpose of this study was to provide a theoretical evaluation of the benzene ring, and three methyl groups (CH_3) that give the chemical its name (mesitylene, or C_9H_{12}) using quantum computation. The theoretical characteristics of the research were investigated using Gaussian software (DFT)/B3LYP employing 3-21G STO cc-pVDZ VDD basis sets. The mesitylene structures' shape was then optimized using this knowledge. The calculations for the electronic properties, including excitation energies, wavelengths, E_{HOMO} and E_{LUMO} energies, (DOS), Molecular Orbital Theory (MOT), electronic charge destruction, FT-IR, and the RAMAN spectrum, were carried out by DFT. The thermochemistry results, which include entropy (S), molar heat capacity (Cv), and thermal energy (E) complement the electronic properties. The STO/B3LYP base set has an excellent value for the BG energy, which is calculated to be 6.562 eV. This result agrees with previous research 6.22 eV.

ARTICLE INFO

Keywords:
Mesitylene
DOS
HOMO, and LUMO
FT-IR
RAMAN
Thermochemistry

Received: 2024-02-26
Accepted: 2024-04-05
ISSN: 2651-3080
DOI: 10.54565/jphcfum.1350445

1. INTRODUCTION

Mesitylene is an aromatic hydrocarbon, known as 1,3,5-trimethylbenzene, with the molecular formula C_9H_{12} [1]. Mesitylene is readily accessible since it is a benzene derivative that may be manufactured from coal tar [2, 3]. It is composed of a benzene ring with three methyl ($-CH_3$) groups attached at meta-positions 1, 3, and 5 [4, 5]. Mesitylene is an essential and emblematic part of the C3v-type high symmetry [6, 7]. However, Mesitylene is a colorless liquid at room temperature and has a distinct aromatic odor. The melting point is around -45.7°C, but the boiling point is approximately 165.1°C. Mesitylene is relatively insoluble in water due to its hydrophobic nature, but it is soluble in organic solvents [8, 9].

Mesitylene is commonly used as a solvent in various industrial and laboratory applications due to its solvency properties. It can also be used as a starting material in the synthesis of other chemicals and compounds [10, 11]. Mesitylene has been proposed as a useful ingredient in the development of simple hydrocarbon mixtures that quantitatively mimic the gas-phase combustion behavior of real liquid transportation fuels as a model or surrogate fuel. To aid in its implementation, a novel chemical kinetic model for the combustion of mesitylene was developed after its numerous combustion characteristics were characterized experimentally [12]. The experimentally determined laminar burning velocities, shock ignition delays, and oxidative reactivity profiles of a high-pressure flow reactor are provided [13, 14]. However, alcohols are often extracted using conventional solvents like mesitylene, to manufacture the porous carbons that have been so important in the adsorptive carbon capture process, that it is recommended that it be used as the starting material. In addition, it is used in organic synthesis (for making things like high-octane additives to liquid fuels and antioxidants and thermal stabilizers for polymers, plant growth regulators, color intermediates, pollutant scavenging agents, and explosives, among other things) [15, 16]. utilized by several sectors, including the petrochemical, plastics, and printing sectors [17].

An oxidation model for mesitylene was created to foretell the fuel's decomposition and the emergence of aliphatic and single-ring aromatic hydrocarbons. When burned, it releases harmful pollutants and is a neurotoxic compound [17], so they are emitted into the atmosphere by

evaporation and vehicle tailpipes [18]. Infrared spectroscopy was used to examine the stability of mesitylene in the presence of oxygen at temperatures below 670 K, even at timeframes (1.8 s) and pressures (12.5 atm) far longer than those encountered in the vaporization apparatuses [19].

DFT method was used to model and analyze the electronic structure and properties of mesitylene. When applied to mesitylene, DFT calculations would involve predicting various aspects of the molecule's behavior, such as its geometry, electronic structure, vibrational frequencies, and other properties. Using DFT to gain insights into the behavior of mesitylene on a molecular level. This can include understanding how the molecule interacts with other molecules, surfaces, or external forces, as well as predicting its spectroscopic properties [20-23].

On the other hand, when mesitylene underwent heat interaction with diazoacetates, only the resultant byproducts of carbene insertion into the C-H bond of mesitylene were generated. Computational simulations using (DFT) revealed that the thermal reaction between diazoacetates and benzene led to a distinct preference in product formation [24-26]. Both the HOMO and LOMO orbitals belonging to the π* orbital system of mesitylene were found to have single electron occupancy. The reduction of mesitylene is evident from an electron population of 0.7 on the aromatic ring. These characterizations align with the molecular structures of these compounds, which possess notably more nonplanar arene rings as indicated by density functional theory calculations [27, 28].

The purpose of this research is to determine the best molecular structure of mesitylene as well as its vibrational amplitudes and chemical modifications. Using the DFT method, and B3LYP global quantum chemical processes, a complete analysis included theoretical data. In this study, the calculated findings supported previous experimental results, including FT-IR, Raman, MOT, NMR, and UV spectra.

2. MATERIAL AND METHOD

In this current project, the quantum program Gaussian 5.0.9W performed all Mesitylene (C_9H_{12}) atomic calculations and 3-D gas phase simulations. The program known as the Gauss View 5.0 package was employed to estimate the initial geometries of the chemical compounds. Additionally, the Gaussian 09W was used for output computations with a B3LYP method, and a variety of basis sets (including 3-21G, STO, cc-Pvdz, and SDD) was used to optimize the geometry of the Mesitylene compound.

Through performing single-point calculations, we were able to assess both the global and local characteristics of the optimized molecules. Specific factors significantly impact the reactivity of chemicals. The below e parameters are frequently detected as the eigenvalues of the amount of energy of the (E_{HOMO}), (E_{LUMO}), the band gap of energy (E_{gap}), the ionization energy (IE), the electron affinity (EA), the absolute electronegativity ($\boldsymbol{\chi}$), the global hardness (η), the global softness (S), the global electrophilic ($\boldsymbol{\omega}$), the electro accepting ω^+, electro donating, ω^-, fraction of electrons transferred [29] and a fraction of electrons transfer ($\Delta \boldsymbol{N_{max}}$) [29-31] [1,2,3].

IE and EA are the difference between neutral and cation and neutral and anion [33,34]. The ionization energy and affinity for electrons were calculated by applying equations (1) and (2) [30, 32-34]:

$$\boldsymbol{IE = E(N-1) - E(N)} \quad (1)$$

And

$$\boldsymbol{EA = E(N) - E(N+1)} \quad (2)$$

Here the energy (E) of the neutral is denoted by (N), the E of the cation is denoted by (N-1), and the E of the anion is denoted by (N+1).

The band gap energy, denoted by the symbol (E_{gap}), is the difference in energy that exists between the two states denoted by E_{LUMO} and E_{HOMO} as shown in equation (3):

$$\Delta \boldsymbol{E_{Gap}(eV = E_{HOMO} - E_{LUMO})} \quad (3)$$

Equation 4 was used in the calculation to get the absolute chemical hardness [35-39]:

$$\eta = \frac{\boldsymbol{IE - EA}}{\boldsymbol{2}} = \frac{\boldsymbol{E_{HOMO} - E_{LUMO}}}{\boldsymbol{2}} \quad (4)$$

In equation (5), molecular softness characterizes an atom or set of atoms' electron-receiving areas:

$$\boldsymbol{S} = \frac{\boldsymbol{1}}{\eta} = \frac{\boldsymbol{2}}{\boldsymbol{E_{LUMO} - E_{HOMO}}} \quad (5)$$

According to equation (6), the $\boldsymbol{\chi}$ is a significant part of the overall reactivity and is referred to as the negative value of the chemical potential:

$$\boldsymbol{\chi} = \frac{\boldsymbol{IE + EA}}{\boldsymbol{2}} = \frac{\boldsymbol{-(E_{HOMO} + E_{LUMO})}}{\boldsymbol{2}} \quad (6)$$

The following equation (7) is the formula that is used to calculate the electronic chemical potential based on the electronic molecular orbital (EMO) energies. Where in this particular investigation did HOMO investigate in 33 EMO, and where LUMO appear in 34 EMO:

$$\boldsymbol{\mu} = \frac{\boldsymbol{E_{HOMO} + E_{LUMO}}}{\boldsymbol{2}} \quad (7)$$

By using equation (8), we were able to calculate the magnitude of the greatest energy drop that occurred as a direct consequence of the movement of electrons from the donor to the acceptor. In addition to this, the global electrophilicity ($\boldsymbol{\omega}$) index of a chemical species is obtained by the process of dividing the square of the electronegativity ($\boldsymbol{\chi}$) by the chemical hardness. This definition was provided by Parr and colleagues [40-43]:

$$\boldsymbol{\omega} = \frac{\boldsymbol{\mu^2}}{\boldsymbol{2}} \times \boldsymbol{S} = \frac{\boldsymbol{\mu^2}}{\boldsymbol{2\eta}} \quad (8)$$

Equations (9), and (10) were used to calculate the amount of electrons electro donating and electro accepting, respectively. Where $\boldsymbol{\omega^+}$ denotes the capacity of the

molecular system to accept charges, while ω^- stands for the ability to provide charges to other molecules.

$$\omega^+ = \frac{EA^2}{2(IE - EA)} \quad (9)$$

$$\omega^- = \frac{IE^2}{2(IE - EA)} \quad (10)$$

We make note of the fact that a greater value for ω^+ implies that a system can absorb charge (accept charge), also lower value for ω^- suggests that it is a more effective electron donor.

We have also made use of the following equation (11)) to determine the maximum number of electrons that may be obtained by an electrophile utilizing the use of the quantum chemical technique:

$$\Delta N_{max} = \frac{-\mu}{\eta} \quad (11)$$

3. RESULTS AND DISCUSSIONS

The ground energies that have been determined for the Mesitylene (C_9H_{12}) molecule compound after they have been optimized. Molecules were optimized using the DFT technique, utilizing the B3LYP functional with the 3-21G basis set. In the first step of advantageous geometry optimization methods for this approach, the energy that corresponds with a certain beginning compound shape is determined as seen in Table 5, below is illustrated as an example.

3.1. Geometry Optimization

The ground energies that have been determined for the Mesitylene (C_9H_{12}) molecule compound after they have been optimized. Molecules were optimized using the DFT technique, utilizing the B3LYP functional with the 3-21G basis set. In the first step of advantageous geometry optimization methods for this approach, the energy that corresponds with a certain beginning compound shape is determined as seen in Table 1, and Table 3 below is illustrated as an example.

	DFT/ B3LYP/ 3-21G Basis set		
Symbol	**Bond length (A°)**	**Symbol**	**Bond length (A°)**
C1-C2	2.4162603	H10-C11	2.1404318
C2-C3	2.4161826	C11-H12	1.0700000
C3-H4	1.0996562	H12-H13	1.0700000
H4-H5	1.0996784	H13-H14	1.0700000
H5-H6	1.0996048	H14-C15	2.1406585
H6-C7	2.1406288	C15-H16	1.0700000
C7-H8	1.0700000	H16-H17	1.0700000
H8-H9	1.0700000	H17-H18	1.0700000
H9-H10	1.0700000	C20-C21	1.0700000
Symbol	**Average Bond length (A°)**		
1^{st} $CH3_{methyl}$	**average**	5.35062	
1^{nd} $CH3_{methyl}$		5.35043	
2^{rd} $CH3_{methyl}$		5.35065	

Table 1 Bond length for the Mesitylene structure

Table 2 Thermal chemistry using standard temperature 298.150 K

	DFT/ B3LYP/ 3-21G Basis set		
Symbol	**Bond Angle (°)**	**Symbol**	**Bond Angle (°)**
C3-C2-H4	149.9779251	C11-H12-H13	137.5288543
H5-C4-C3	149.9758000	H12-H13-H14	105.7798980
H5-H6-C7	115.6541115	H13-H14-C15	55.6581836
H6-C7-H8	137.4685051	C2-C1-C3	60.0004016
C7-H8-H9	137.4685051	C15-H16-H17	79.3409610
H8-H9-H10	105.8620193	H14-C15-H16	137.4442982
H9-H10-C11	115.6713750	H16-H17-H18	105.8950702
H10-C11-H12	79.3900000	H17-H18-H19	34.3629146
H19-C20-C21	34.3589229	H18-H19-C20	34.3575107

3.2. Thermal Chemistry

The parameters associated with thermodynamics provide information that is both useful and additional to the title molecule. The science of thermochemistry focuses on the energy shifts and exchanges that occur with applied chemical and physical processes. The study of how energy is transferred during chemical processes is known as thermochemistry [44-46]. DFT was used in this analysis to evaluate the thermodynamic characteristics parameters of this molecule using ground state, and STO basis set at standard temperature 298.15 K.

These parameters include entropy (S), molar heat capacity (Cv), and thermal energy (E). Table 2 shows how the polarity of the solvent modifies the S, E, and molar Cv values.

Table 3 Bond angle is important characteristic for the Mesitylene structure.

Calculation of Parameters	**E (Thermal) kcal/mol**	**Cv cal/mol.K**	**S cal/mol.K**
Total	130.531	33.872	98.128
Electronic	0.000	0.000	0.000
Translational	0.889	2.981	40.264
Rotational	0.889	2.981	29.245
Vibrational	128.754	27.910	28.620

3.3. Band Gap Energy

The findings of estimating the energy gap (Egap) for Mesitylene (C_9H_{12}) are shown in Table 4 and Figure 1. During the computations, an appropriate DFT was used to achieve a precise assessment of the different band gap

energies, which were (3-21G, 6.633 eV), (STO, 6.562 eV, cc-Pvdz, 5.3579 eV), and (SDD, 5.520 eV). Figure 1 illustrated HOMO, and LUMO energy for the compound.

In this instance, the STO basis set has a larger HOMO energy, which translates to a greater reactivity of the compound in electrophile processes. While, on the other hand, the 3-21G basis set has a HOMO energy that is smaller BG (-6.270 eV), which indicates that it represents a molecule that becomes less reactive in nucleophile operations. Because E_{LUMO} has a negative quantity, it has been determined that mesitylene (C_9H_{12}) has a greater stable than E_{HOMO} the compounds [30, 47].

Table 4 Energy calculation of methylene via the DFT technique and the B3LYP basis set

In this instance, the STO basis set has a larger HOMO energy, which translates to a greater reactivity of the compound in electrophile processes. While, on the other hand, the 3-21G basis set has a HOMO energy that is smaller BG (-6.270 eV), which indicates that it represents a molecule that becomes less reactive in nucleophile operations. This finding was completely confirmed by the prior work on the energy estimate of Mesitylene [48]. Because E_{HOMO} has a positive quantity, it has been determined that mesitylene (C_9H_{12}) has a greater unstable than E_{LUMO} compounds [30, 49].

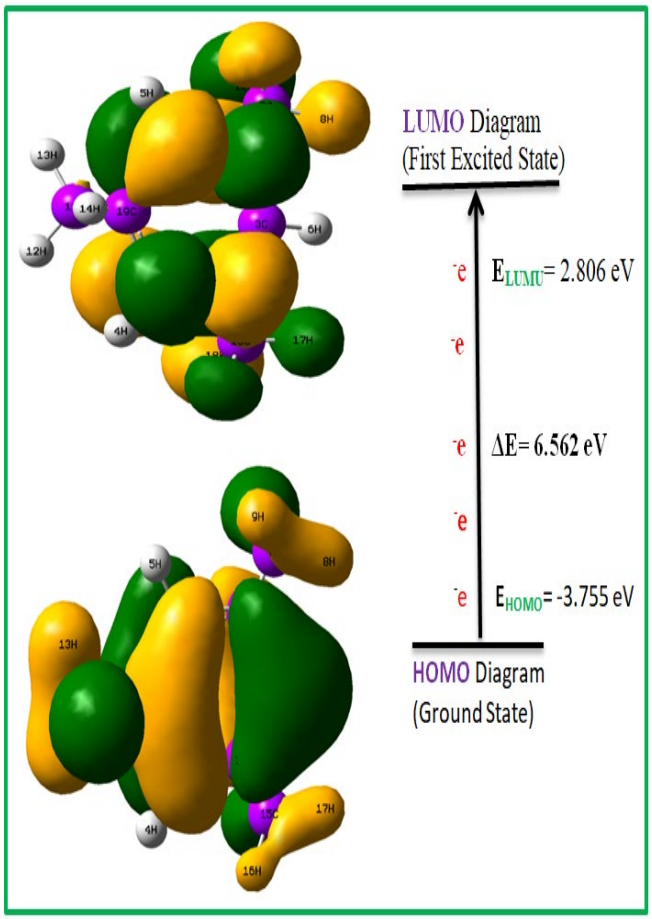

Figure 1 HOMO and LUMO diagram for Mesitylene

3.4. Ionization Energy (IE) and Electron Affinity (EA)

The IE and EA values that were determined using the difference approach are shown in Figure 2 according to **Table 5** the research demonstrates that the STO basis set has ionization potential values (3.755159) that are lower than those of other basis sets. This discovery provides greater support to the idea that the substance in examination is an electron donor. It has been shown that the Mesitylene (C_9H_{12}) molecule has the greatest EA value when employing the cc-pVDZ basis set, which is evidence of its electron acceptor capacity [30].

Table 5 Theoretical calculation of IE, and EA parameters for Mesitylene structure.

Energy	MOs Theory	Theoretical Calculation Basis Set				Related article [48]
		3-21G	STO	cc-pVDZ	VDD	
EHOMO	33	-6.270	-3.755	-5.338	-5.313	
ELUMO	34	0.362	2.806	0.0193	0.206	
ΔE (eV)		6.633	6.562	5.3579	5.520	6.22 eV
E(RB3LYP) (a.u)		-348.28	-344.97	-349.41	-349.31	
E(RB3LYP) (a.u)		-348.28	-344.97	-349.41	-349.31	

Basis set	IE (eV)	EA (eV)
3-21G	6.270572	-0.36273
STO	3.755159	-2.80685
cc-pVDZ	5.338585	-0.01932
SDD	5.313823	-0.20653

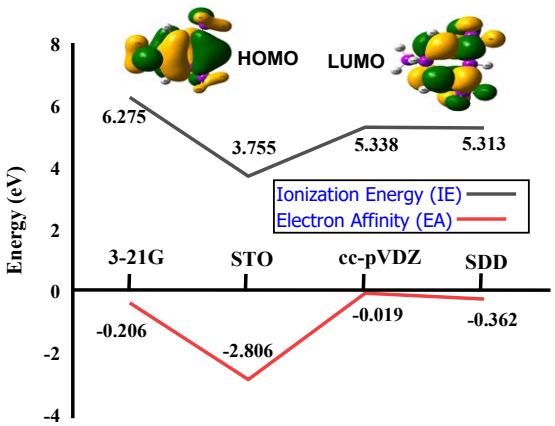

Figure 2 Relation IE and EA as energy functions for Mesitylene

3.5. Dipole Moment

The dipole moment may be defined as the total of the sums of the products of the system's electric charges by their respective radius vectors. The dipole moment, denoted by the symbol (μ), is a significant electrical characteristic that may be used to determine the overall polarity of a molecule. In some molecules, the μ may be found even when there is no external field present. The DFT-B3LYP/6-31G (d) basis set is used in Table 6, where the dipole moment values of Mesitylene (C_9H_{12}) are shown for comparison. The significant polarity of the molecules is almost certainly the compound [30, 50-52].

According to the research that has been done, chemicals that have substantial dipole moments are more reactive, which results in an important rise in the amount of substance that may be removed. The compound has a high dipole moment value (=0.1785 Debye, when calculated using the cc-pVDZ basis set) when compared to the values of other basis sets, which is much higher. A big dipole moment indicates that the molecule has a significant amount of electronic charge polarity, which is the basic cause of the chemical reaction [53, 54].

Table 6 Mesitylene (C_9H_{12}) Dipole Moment Values Calculated using DFT-B3LYP and other Basis Sets

Basis set	Total Dipole Moment (Debye)
3-21G	**0.0477**
STO	**0.1034**
cc-pVDZ	**0.1785**
SDD	**0.1762**

3.6. Hardness (η) and Softness (S)

Mesitylene (C_9H_{12})'s global hardness and softness statistics are shown in Table 7, and Figure 3 with energy function, along with the reagent that was investigated. It is necessary to have an understanding of a molecule's global S and η to better understand its molecular stability and chemical reactivity. Chemical hardness is a term for assessing chemical reactivity and defining a system's charge transfer resistance. The lower the values, the more likely an electron transfer will occur in the system. A rigid molecule typically has a wider energy gap, while a soft molecule typically has a narrower one [45].

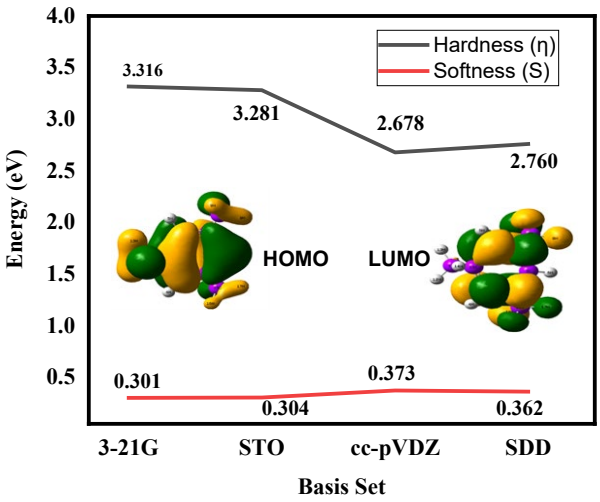

Figure 3 Graphical function of Molecular Hardness (η), and Softness (S) with energy function

From the data presented in Table 7, it has been observed that the Mesitylene (C_9H_{12}) molecule has the lowest hardness (η = 2.678952) and the highest softness (S = 0.37328) using the cc-pVDZ basis set method, which explains their higher reactivity compared with the other molecule basis set.

Table 7 Molecular Hardness (η) Softness (S) using DFT/B3LYP method

Basis set	Hardness (η)	Softness (S)
3-21G	3.316649	0.301509
STO	3.281002	0.304785
cc-pVDZ	2.678952	0.37328
SDD	2.760178	0.362295

3.7. Global Electrophilicity (ω) and the Nucleophilicity Index (N)

By analyzing the nucleophilicity, and electrophilicity index that the CDFT offers for the compounds in their ground state, one can easily predict the electrophilic-nucleophilic interactions that will take place in the structure of the transition state [40]. Electrophiles (ω) are molecules or atomic particles or ions that have the capability of accepting electron pairs, while nucleophiles are chemical atoms or chemical molecules that can donate electron pairs. ω may be (+) or a natural charge, while **N** often has a (-) charge due to its nature. Mesitylene (C_9H_{12}) molecule has the greatest value of electrophilicity index (= 5.589eV) utilizing a 3-211G basis set. This is in comparison to the STO (= 0.8429.776 eV), cc-pVDZ (= 5.300), and SDD (= 4.918eV). This can be seen in Table 8. On the other hand, the energy difference between 3-21G is much greater (-6.63 eV). Analyzing the electroaccepting, ω^+, and electrodonating, ω^- , indices given in Table 8 reveals a similar trend, ω^+ (3.48) > ω^+ (3.48) > ω^+ (0.009)> ω^+ (0.003) with using 3-21G, STO, cc-pVDZ, and SDD

basis set. It follows that a higher value of ω^+ correlates to a stronger capacity of gaining charge, whereas a lower value of ω^- value of a system makes it an excellent electron donor [55]. This is because + and – are inversely proportional to each other. Based on the information in Table 8, the nucleophilicity index of Mesitylene (C_9H_{12}) (ΔN_{max} = 1.989 eV) of cc-pVDZ basis set is greater than other diners.

Table 8 Global ω, ω^+, ω^-, and ΔN_{max} for **Mesitylene**

Basis set	ω	ω^+	ω^-	ΔN_{max}
3-21G	5.589	0.009	2.963	1.835
STO	0.842	0.600	1.074	0.716
cc-pVDZ	5.300	3.48	2.659	1.989
SDD	4.918	0.003	2.557	1.887

3.8. Chemical Electronegativity (χ), and Electron Potential (μ)

Electronegativity or (χ) is the capacity of an atom or molecule to attract an electron from another atom or molecule. Electronegativity is a strong notion that may immediately assume the direction in which charge is transferred as well as the polarity of bonds. The direction in which electrons move is determined by the chemical potentials. In our theory, the chemical μ potential can be defined by changing electronegativity, chemical hardness, electronic attraction within a molecular structure, and core-level sensitivity to density of electrons shifts [56].

The information that is shown in Table 9, and Figure 4 demonstrates that the chemical potentials have the exact opposite relationship to the electronegativities as expected. In addition to this, when compared to the other reactants, the electronegativity value of the STO basis set is the minimum it can be (χ = 2.351737 eV). This is because of the greater atomic size of the element, which leads to a smaller value for its chemical electronegativity. According to Table 9, the molecule Mesitylene has the greatest value of chemical potential invested on an STO basis (μ =-2.35174 eV). A summary of the findings presented here, the molecule Mesitylene has a nucleophilic quality.

Table 9 χ, and μ for Mesitylene using various basis set

Basis set	χ	μ
3-21G	6.089209	-6.08921
STO	2.351737	-2.35174
cc-pVDZ	5.328925	-5.32892
SDD	5.210556	-5.21056

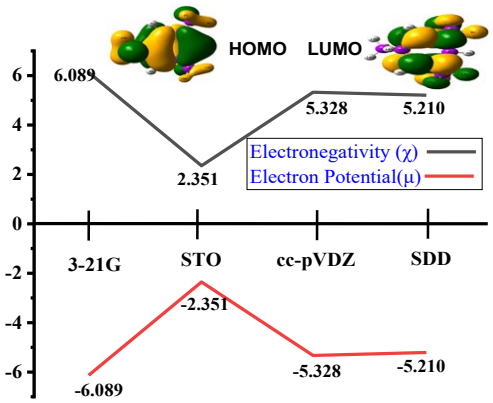

Figure 4 Graph showing the electronegativity and a study of the chemical potential using DFT/B3LYP

3.9. Electronic Density of State (DOS)

The density of state (DOS) graphs for the examined compounds are shown at B3LYP/ 6-31G and may be seen in Figure 5. This graph shows the difference in energy between two different energy levels, HOMO and LUMO. These energy levels are represented by green and red lines, respectfully. In a quantum mechanical system, the electronic DOS is a measurement that determines how "packed" electrons are at different energy levels. The interaction between molecules splits molecular levels into related levels, providing the basis for atomic band structure, and DOS calculations [57-59].

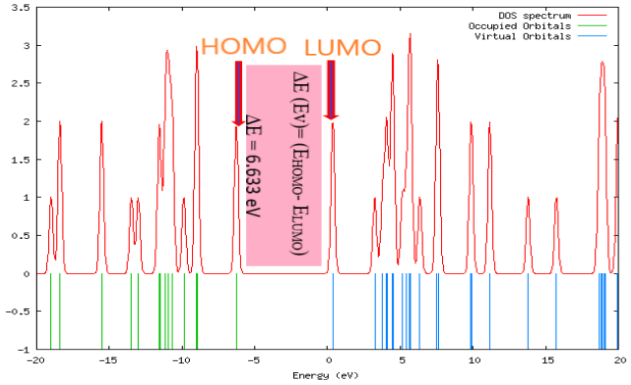

Figure 5 The DOS diagram using DFT/3-21G basis set

The DOS diagram provides a graphic representation of the energy that is accessible for transitions like chemical thermal excitation. An electron that is located in a valence band (VB), which is a band that is occupied and is located below the Fermi energy, has the potential to take on momentum and energy and move into a conduction band (CB), which is a band that is unoccupied and is located above the Fermi energy [59-62]. In this new state, the energy difference between the final and initial states is equal to the energy that was absorbed. The DOS of HOMO in the compounds that were investigated is shown in Figure 5. The DOS maps often confirm that the compounds undergo a density shift from the source areas to the center region [30].

3.10. FT-IR, and RAMAN Spectroscopy

The stretching and bending vibrations of the ring are of essential importance and are very different from the molecule aromatic ring in its own right. FT-IR and RAMAN spectra were assigned to our constituents with the help of the DFT/ 3-21G basis set as shown in Figure 6, and Figure 7. C-H symmetric stretching was investigated and its findings were obtained using FT-IR at a wavelength of 3179.33 cm^{-1} for this particular investigation, while asymmetric stretching was observed utilizing a range that went from 31175.07 to 3174.02 cm^{-1}, and C-H asymmetric bending was found to be in the range of 225.66, 723.93, and 1366.24 cm^{-1} at the same time.
The $C\text{-}CH_3$ vibrations are significant modes for the compounds that included groups of methyl. These modes are often distorted by C-H in-plane bending vibrations. In the investigation of the $C\text{-}CH_3$ vibrational bending, the range of wavenumbers from 468.01 to 272.88 cm^{-1} was considered. Also, CH_3 symmetrical stretching was around 3043.36 to 3044.33 cm^{-1} wavenumber, and asymmetrical stretching was 3097.56 to 3097.15 cm^{-1} wavenumber. Finally, asymmetric bending was the range of 1558.66 cm^{-1}, and asymmetric bending was 1101 to 1097.66 cm^{-1}. Our findings are in the most full agreement with the previous research[63].

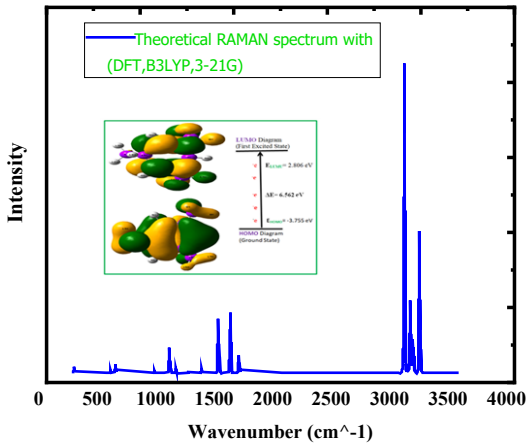

Figure 6 RAMAN spectrum using DFT method

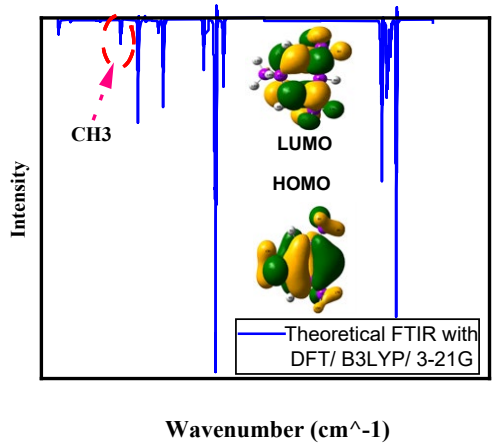

Figure 7 FT-IR spectrum using DFT method/ B3lyp, and 3-21G basis set for Mesitylene

3.11. Mulliken Atomic Charge

Application Quantum mechanical computations of the molecular structure rely significantly on atomic charges. In THIS research, the DFT/B3LYP technique and the 6-STO basis set are used to calculate the Mulliken atomic charges of mesitylene, and benzene. We selected benzene and these three compounds for further study based on the quantity of methyl groups, or CH_3 groups, that were linked to the benzene ring. In Table 10, the Mulliken molecular charges of all the molecules from benzene to mesitylene compound are mentioned. According to the findings, altering the structure of the aromatic ring results in a change in the distribution of electron density. The outcome of the atomic charge calculations is presented and analyzed here to demonstrate the influence of groups of methyl. The carbon atoms connected to the methyl group have various charges based on the amount of methyl groups [64].

Table 10 Mulliken charges density

atomic	Mulliken charges	atomic	Mulliken charges
1-C	-0.153105	12-H	0.197034
2-C	-0.153121	13-H	0.196435
3-C	-0.151538	14-H	0.240734
4-H	0.137235	15-C	-0.705189
5-H	0.137307	16-H	0.1958
6-H	0.136831	17-H	0.1974
7-C	-0.705129	18-H	0.2404
8-H	0.196763	19-C	0.0885
9-H	0.195368	20-C	0.0875
10-H	0.240147	21-C	0.0878
11-C	-0.706037	12-H	0.1973

According to our findings, which are shown in Table 11, the relative magnitudes of the charges of hydrogen atoms and groups of methyl in all CH_3 molecules are essentially identical. Nonetheless, the findings demonstrate that a symmetrical redistribution of electron density occurs upon phenyl ring replacement with CH_3 groups. In particular, the symmetry of the CH_3 groups for the molecule results in a symmetric distribution of the molecule's charge (C is negatively charged, while 3H is positively charged). As a consequence of the presence of the CH_3 groups, the carbon atoms displayed a variety of charges [64].

3.12. Molecular Orbital Theory (MOT)

The density functional theory, sometimes known as DFT, has several significant applications in the field of chemistry, and the calculation of chemical, and physical parameters. In this present study one by one we discuss the significance of the DFT method. A chemical process consists of nuclei and electrons, such as atoms, molecules, ions, or radicals, interacting. It is helpful to link (E_{HOMO}, E_{LUMO}, E_{gap}, IE, EA, χ, η, S, ω, ω+, ω-, with molecular orbital (MO), which may be identified as MO, to derive alternative approximations to the values of chemical parameters [65].

Table 11. Alpha MOs theory using DFTBELYP/ 3-21G basis set

Alpha MOs theory							
MOs	**Energy**	**MOs**	**Energy**	**MOs**	**Energy**	**MOs**	**Energy**
1	-10.1293619000	35	0.0134392916	57	0.5782995650	85	1.0918312100
2	-10.1293517000	36	0.1193482430	58	0.6857833000	86	1.0923054400
3	-10.1292861000	37	0.1390652900	59	0.6912058520	87	1.0971116800
4	-10.1144442000	38	0.1484785450	60	0.6933043260	88	1.1024373700
5	-10.1144398000	39	0.1506965730	61	0.7002725710	89	1.1471620700
6	-10.1143777000	40	0.1635942590	62	0.7008549690	90	1.1474400100
7	-10.1127062000	41	0.1639143130	63	0.7333484220	91	1.2634770700
8	-10.1126890000	42	0.1665207910	64	0.7345102740	92	1.270042840
9	-10.1123744000	30	-0.3306182480	65	0.7459336430	93	1.4272223100
10	-0.8567391220	31	-0.3296031290	66	0.7464588180	94	1.4273568700
11	-0.7755706210	32	-0.2304432640	67	0.7924765120	96	1.5509880700
12	-0.7755408500	33	-0.2304367430 = **HOMO**			$\Delta E\ (Ev) = (E_{HOMO} - E_{LUMO})$	
13	-0.6983808300	34	0.0133272112 = **LUMO**			ΔE = 6.633 eV	
14	-0.6762158880	42	0.1665207910	68	0.7951091330	96	1.5511080900
15	-0.6762102030	43	0.1895847940	69	0.8258445720	97	1.5955656900
16	-0.5705293930	44	0.2002490810	70	0.8264079260	98	1.6186555400
17	-0.5704999730	45	0.2079574630	71	0.8872729540	99	1.6190327600
18	-0.4955722470	46	0.2092979740	72	0.8916430800	100	1.9060749100
19	-0.5704999730	47	0.2097129910	73	0.9221924020	101	1.9201383500
20	-0.4258661810	48	0.2331668770	74	0.9302490170	102	1.9202694100
21	-0.4237908520	49	0.2763011540	75	0.9390765040	103	1.9879491200
22	-0.4098427680	50	0.2798408860	76	0.9404428800	104	1.9893366000
23	-0.4092925760	51	0.2800198110	77	0.9598564780	105	2.4923784500
24	-0.4020202610	52	0.3625544790	78	0.9659831080	Note	
25	-0.4019368120	53	0.3634298090	79	0.9870857550	**HOMO= (1 to 33) Molecular Orbital**	
26	-0.3928264480	43	0.1895847940	80	1.0427292100		
27	-0.3927735880	54	0.4100945020	82	1.054778980		
28	-0.3630533170	55	0.4102438290	83	1.0819174400	**LUMO=(34 to 105) Molecular Orbital**	
29	-0.3306182480	56	0.5068676270	84	1.0856967600		

As a result of the fact that the gap in MOT also reflects the difference in energy between the ground state and the first excited state of the same multiplicity, numerous interesting inferences may be inferred from this information. Table 11 indicates alpha MOs theory using the DFT/ B3LYP/ 3-21G basis set.

According to the principles of quantum mechanics, the majority of chemical reactions involve the mixing of wave functions representing excited states with wave functions representing ground states [66]. A smaller energy gap is preferable for easing simple interaction. The DFT may create the whole border MO of reactivity of chemicals [67]. Electron transport between HOMOs and LUMOs during the reaction.

4. Conclusion

In the present research, 3-21G, STO, cc-pVDZ, and SDD basis sets were utilized for the application of the density functional theory (DFT/B3LYP) method using the Gaussian 09W programme. The investigation of the chemical reactivity of the mesitylene compound has been the primary focus of this research. The predicted BG energy of 6.562 eV using the STO/B3LYP basis set is an excellent value. This result agrees with the 6.22 eV found in the literature. Since E_{LUMO} has a negative amount, mesitylene (C9H12) is more stable than E_{HOMO}. Using the cc-pVDZ basis set, the compound's dipole moment is 0.1785 Debye, which is substantially greater than other basis sets. A high dipole moment suggests a molecule with high electrical charge polarity. All IR and Raman results were validated by computational results, compared to actual data. Vibrational wavenumbers, electrical characteristics, and chemical shift values confirmed past research.

REFERENCES

[1] D. Gin, M. Cader, J. Sams, F. Aubke, 1, 3, 5-Trimethylbenzene (mesitylene) adducts with selected tin (II) compounds: the syntheses of Sn (SO3F) 2• C9H12 and Sn (SbF6) 2• 2C9H12, Canadian journal of chemistry, 68 (1990) 350-355.

[2] R. Verma, P. Dehury, A. Bharti, T. Banerjee, Liquid-liquid extraction, COSMO-SAC predictions and process flow sheeting of 1-butanol enhancement using mesitylene and oleyl alcohol, Journal of Molecular Liquids, 265 (2018) 824-839.

[3] O. Rebaz, R.F. Rashid, K. OTHMAN, Exploring The Synthesis of 1, 2, 4-Triazole Derivatives: A Comprehensive Review, Journal of Physical Chemistry and Functional Materials, 6 43-56.

[4] J.G. Baragi, M.I. Aralaguppi, Excess and deviation properties for the binary mixtures of methylcyclohexane with benzene, toluene, p-xylene, mesitylene, and anisole at T=(298.15, 303.15, and 308.15) K, The Journal of Chemical Thermodynamics, 38 (2006) 1717-1724.

[5] J.A. Al-Kandary, A.S. Al-Jimaz, A.-H.M. Abdul-Latif, Excess molar volumes and refractive indices of (methoxybenzene+ benzene, or toluene, or o-xylene, or m-xylene, or p-xylene, or mesitylene) binary mixtures between T=(288.15 to 303.15) K, The Journal of Chemical Thermodynamics, 38 (2006) 1351-1361.

[6] S.-C. Qi, Y. Liu, A.-Z. Peng, D.-M. Xue, X. Liu, X.-Q. Liu, L.-B. Sun, Fabrication of porous carbons from mesitylene for highly efficient CO2 capture: A rational choice improving the carbon loop, Chemical Engineering Journal, 361 (2019) 945-952.

[7] L. AHMED, N. BULUT, O. KAYGILI, O. Rebaz, Quantum Chemical Study of Some Basic Organic Compounds as the Corrosion Inhibitors, Journal of Physical Chemistry and Functional Materials, 6 (2023) 34-42.

[8] T.L. Seidl, The Preparation of Diaryliodonium Salts for Application in Arylation Chemistry, (2018).

[9] M.R. Lutz Jr, Application of Synthetic Organic and Medicinal Chemistry Toward Medical Advances in Cancer, Antibiotics, and Drug Delivery, Loyola University Chicago, 2018.

[10] R.A. OMER, R.A. Mustafa, S. Salih, W. Hamad, S. Taher, Synthesis of A New Series of Benzothiazole Compounds and Study of Their Liquid Crystal Properties, Passer Journal of Basic and Applied Sciences, 5 (2023) 78-84.

[11] K. Kosrat, O. Rebaz, S. TAHER, W.M.H. HAMAD, Dissociation Constant Studies of 2-Substituted 4-Formylbenzoic Acid based on Conductometric Parameters using Fuoss-Hsia Theories, International Journal of Thermodynamics, 26 (2023) 1-10.

[12] R.A. Omar, P. Koparir, K. Sarac, M. Koparir, D.A. Safin, A novel coumarin-triazole-thiophene hybrid: synthesis, characterization, ADMET prediction, molecular docking and molecular dynamics studies with a series of SARS-CoV-2 proteins, Journal of Chemical Sciences, 135 (2023) 6.

[13] P. Diévart, H.H. Kim, S.H. Won, Y. Ju, F.L. Dryer, S. Dooley, W. Wang, M.A. Oehlschlaeger, The combustion properties of 1, 3, 5-trimethylbenzene and a kinetic model, Fuel, 109 (2013) 125-136.

[14] R.A. Omer, P. Koparir, M. Koparir, Synthesis, experimental and theoretical characterization with inhibitor activity for 1, 2, 4-triazole derivatives, Indian Journal of Chemistry (IJC), 61 (2022) 1278-1287.

[15] L. Faba, J. Gancedo, J. Quesada, E. Diaz, S. Ordonez, One-pot conversion of acetone into mesitylene over combinations of acid and basic catalysts, Acs catalysis, 11 (2021) 11650-11662.

[16] G.D. Yadav, N.S. Asthana, Kinetics and mechanism of selective monoacylation of mesitylene, Industrial & engineering chemistry research, 41 (2002) 5565-5575.

[17] E.Y. Choi, Y. Kim, K. Seff, Crystal structure of a mesitylene sorption complex of dehydrated fully Ca2+-exchanged zeolite X. sorbed mesitylene appears to be significantly nonplanar, The Journal of Physical Chemistry B, 106 (2002) 5827-5832.

[18] M. Huang, Y. Lin, X. Huang, X. Liu, X. Guo, C. Hu, W. Zhao, X. Gu, L. Fang, W. Zhang, Experimental study of particulate products for aging of 1, 3, 5–trimethylbenzene secondary organic aerosol, Atmospheric Pollution Research, 6 (2015) 209-219.

[19] R.A. OMER, P. Koparir, L. Ahmed, Theoretical determination of corrosion inhibitor activities of 4-allyl-5-(pyridine-4-yl)-4H-1, 2, 4-triazole-3-thiol-thione tautomerism, Indian Journal of Chemical Technology (IJCT), 29 (2022) 75-81.

[20] V. Botu, R. Ramprasad, Learning scheme to predict atomic forces and accelerate materials simulations, Physical Review B, 92 (2015) 094306.

[21] R. Omer, P. Koparir, M. Koparir, R. Rashid, L. Ahmed, J. Hama, Synthesis, Characterization and DFT Study of 1-(3-Mesityl-3-methylcyclobutyl)-2-((4-phenyl-5-(thiophene-2-yl)-4H-1, 2, 4-triazol-3-yl) thio) ethan-1-one, Protection of Metals and Physical Chemistry of Surfaces, 58 (2022) 1077-1089.

[22] A.E. Parlak, R.A. Omar, P. Koparir, M.I. Salih, Experimental, DFT and Theoretical Corrosion Study for 4-(((4-ethyl-5-(thiophene-2-yl)-4H-1, 2, 4-triazole-3-yl) thio) methyl)-7, 8-dimethyl-2H-chromen-2-one, Arabian Journal of Chemistry, 15 (2022) 104088.

[23] P. Koparir, R.A. Omar, K. Sarac, L.O. Ahmed, A. Karatepe, T. Taskin-Tok, D.A. Safin, Synthesis, Characterization and Computational Analysis of Thiophene-2, 5-Diylbis ((3-Mesityl-3-Methylcyclobutyl)

Methanone), Polycyclic Aromatic Compounds, (2022) 1-19.
[24] A.V. Serebryannikova, E.E. Galenko, M.S. Novikov, A.F. Khlebnikov, Product selectivity of thermal Buchner reaction of methyl 2-(3-arylisoxazol-5-yl)-2-diazoacetates with benzene, naphthalene and mesitylene, and ring-opening/closing reaction of products, Tetrahedron, 88 (2021) 132153.
[25] R.A. OMER, SYNTHESIS, CHARACTERIZATION AND QUANTUM CHEMICAL CALCULATIONS OF SUBSTITUTED 1, 2, 4-TRIAZOLE DERIVATIVES, (2022).
[26] R.A. Omer, P. Koparir, L.O. Ahmed, Characterization and inhibitor activity of two newly synthesized thiazole, Journal of Bio-and Tribo-Corrosion, 8 (2022) 28.
[27] C.T. Palumbo, D.P. Halter, V.K. Voora, G.P. Chen, A.K. Chan, M.E. Fieser, J.W. Ziller, W. Hieringer, F. Furche, K. Meyer, Metal versus ligand reduction in Ln3+ complexes of a mesitylene-anchored tris (aryloxide) ligand, Inorganic chemistry, 57 (2018) 2823-2833.
[28] O. Rebaz, P. KOPARIR, I. QADER, L. AHMED, Theoretical Determination of Corrosion Inhibitor Activities of Naphthalene and Tetralin, Gazi University Journal of Science, 35 (2022) 434-444.
[29] J.L. Gázquez, A. Cedillo, A. Vela, Electrodonating and electroaccepting powers, The Journal of Physical Chemistry A, 111 (2007) 1966-1970.
[30] M. El Idrissi, S. Elharfaoui, Z. Zmirli, A. Mouhssine, A. Dani, B. Salle, A. Tounsi, K. Digua, H. Chaair, Theoretical and Experimental Study of the Orientation to the Most Effective Coagulant for Removing Reactive Black-5 Dye from Industrial Effluents, Physical Chemistry Research, 12 (2024) 229-248.
[31] M. Belghiti, S. Bouazama, S. Echihi, A. Mahsoune, A. Elmelouky, A. Dafali, K. Emran, B. Hammouti, M. Tabyaoui, Understanding the adsorption of newly Benzylidene-aniline derivatives as a corrosion inhibitor for carbon steel in hydrochloric acid solution: Experimental, DFT and molecular dynamic simulation studies, Arabian Journal of Chemistry, 13 (2020) 1499-1519.
[32] A.E. AKTAŞ, O. Rebaz, M. KOPARIR, Synthesis, Characterization and Theoretical Anti-Corrosion Study for Substitute Thiazole Contained Cyclobutane Ring, Journal of Physical Chemistry and Functional Materials, 5 111-120.
[33] O. Rebaz, L. AHMED, I. QADER, P. Koparir, Theoretical Analysis of the Reactivity of Carmustine and Lomustine Drugs, Journal of Physical Chemistry and Functional Materials, 5 (2022) 84-96.
[34] O. Rebaz, L. AHMED, P. KOPARIR, H. Jwameer, Impact of Solvent Polarity on the molecular properties of Dimetridazole, El-Cezeri, 9 (2022) 740-747.
[35] A. Lesar, I. Milošev, Density functional study of the corrosion inhibition properties of 1, 2, 4-triazole and its amino derivatives, Chemical physics letters, 483 (2009) 198-203.
[36] O. Rebaz, L. AHMED, H. Jwameer, P. KOPARIR, Structural Analysis of Epinephrine by Combination of Density Functional Theory and Hartree-Fock Methods, El-Cezeri, 9 (2022) 760-776.
[37] P. Koparir, R. Omar, M. Koparir, Synthesis and molecular characterization with DFT study of 2-chloro-1-(3-methyl-3-mesityl-cyclobutyl)-ethanone, (2022).
[38] P. Koparir, K. Sarac, R.A. Omar, Synthesis, molecular characterization, biological and computational studies of new molecule contain 1, 2, 4-triazole, and Coumarin bearing 6, 8-dimethyl, Biointerface Res. Appl. Chem, 12 (2022) 809-823.
[39] L. AHMED, O. Rebaz, 1H-pyrrole, furan, and thiophene molecule corrosion inhibitor behaviors, Journal of Physical Chemistry and Functional Materials, 4 (2021) 1-4.
[40] R.G. Parr, L.v. Szentpály, S. Liu, Electrophilicity index, Journal of the American Chemical Society, 121 (1999) 1922-1924.
[41] L. AHMED, O. Rebaz, The Role of the Various Solvent Polarities on Piperine Reactivity and Stability, Journal of Physical Chemistry and Functional Materials, 4 (2021) 10-16.
[42] R.A. OMER, P. Koparir, L. Ahmed, M. Koparir, Computational and spectroscopy study of melatonin, Indian Journal of Chemistry-Section B (IJC-B), 60 (2021) 732-741.
[43] O. Rebaz, P. KOPARIR, I.N. QADER, L. AHMED, Structure reactivity analysis for Phenylalanine and Tyrosine, Cumhuriyet Science Journal, 42 (2021) 576-585.
[44] G.L. Kyriakopoulos, Low Carbon Energy Technologies in Sustainable Energy Systems, Academic Press2021.
[45] I. Tosun, Modeling in transport phenomena: a conceptual approach, Elsevier2007.
[46] L. AHMED, O. Rebaz, Spectroscopic properties of Vitamin C: A theoretical work, Cumhuriyet Science Journal, 41 (2020) 916-928.
[47] L. AHMED, O. Rebaz, Computational study on paracetamol drug, Journal of Physical Chemistry and Functional Materials, 3 (2020) 9-13.
[48] E. Kose, A. Atac, M. Karabacak, P. Nagabalasubramanian, A. Asiri, S.J.S.A.P.A.M. Periandy, B. Spectroscopy, FT-IR and FT-Raman, NMR and UV spectroscopic investigation and hybrid computational (HF and DFT) analysis on the molecular structure of mesitylene, 116 (2013) 622-634.
[49] O. HAMAD, R.O. KAREEM, O.J.J.o.P.C. Kaygili, F. Materials, Density Function Theory Study of the Physicochemical Characteristics of 2-nitrophenol, 6 (2023) 70-76.
[50] V.A. Soifer, Computer design of diffractive optics, Elsevier2012.
[51] O. Rebaz, P. KOPARIR, L. AHMED, M. KOPARIR, Computational determination the reactivity of salbutamol and propranolol drugs, Turkish Computational and Theoretical Chemistry, 4 (2020) 67-75.
[52] R.A. Omer, L.O. Ahmed, M. Koparir, P. Koparir, Theoretical analysis of the reactivity of chloroquine and hydroxychloroquine, (2020).
[53] A. El Kassimi, A. Boutouil, M. El Himri, M.R. Laamari, M. El Haddad, Selective and competitive removal of three basic dyes from single, binary and ternary systems in aqueous solutions: A combined experimental and theoretical study, Journal of Saudi Chemical Society, 24 (2020) 527-544.
[54] L. AHMED, O. Rebaz, A theoretical study on Dopamine molecule, Journal of Physical Chemistry and Functional Materials, 2 (2019) 66-72.
[55] J. Frau, F. Muñoz, D. Glossman-Mitnik, A conceptual DFT study of the chemical reactivity of magnesium octaethylporphyrin (MgOEP) as predicted by the Minnesota family of density functionals, Química Nova, 40 (2017) 402-406.

[56] F. Sessa, M. Rahm, Electronegativity Equilibration, The Journal of Physical Chemistry A, 126 (2022) 5472-5482.
[57] A.A. Korkmaz, L.O. Ahmed, R.O. Kareem, H. Kebiroglu, T. Ates, N. Bulut, O. Kaygili, B. Ates, Theoretical and experimental characterization of Sn-based hydroxyapatites doped with Bi, Journal of the Australian Ceramic Society, 58 (2022) 803-815.
[58] R.O. Kareem, O. Kaygili, T. Ates, N. Bulut, S. Koytepe, A. Kuruçay, F. Ercan, I. Ercan, Experimental and theoretical characterization of Bi-based hydroxyapatites doped with Ce, Ceramics International, 48 (2022) 33440-33454.
[59] R.O. KAREEM, SYNTHESIS AND CHARACTERIZATION OF BISMUTH-BASED HYDROXYAPATITES DOPED WITH CERIUM, (2023).
[60] R.O. Kareem, O. Kaygili, T. Ates, N. Bulut, S. Koytepe, A. Kuruçay, F. Ercan, I.J.C.I. Ercan, Experimental and theoretical characterization of Bi-based hydroxyapatites doped with Ce, 48 (2022) 33440-33454.
[61] F. İsen, O. Kaygili, N. Bulut, T. Ates, F. Osmanlıoğlu, S. Keser, B. Tatar, İ. Özcan, B. Ates, F.J.J.o.t.A.C.S. Ercan, Experimental and theoretical characterization of Dy-doped hydroxyapatites, (2023) 1-16.
[62] A.A. Korkmaz, L.O. Ahmed, R.O. Kareem, H. Kebiroglu, T. Ates, N. Bulut, O. Kaygili, B.J.J.o.t.A.C.S. Ates, Theoretical and experimental characterization of Sn-based hydroxyapatites doped with Bi, 58 (2022) 803-815.
[63] H.F. Hameka, J.O. Jensen, Theoretical studies of the methyl rotational barrier in toluene, Journal of Molecular Structure: THEOCHEM, 362 (1996) 325-330.
[64] E. Kose, A. Atac, M. Karabacak, P. Nagabalasubramanian, A. Asiri, S. Periandy, FT-IR and FT-Raman, NMR and UV spectroscopic investigation and hybrid computational (HF and DFT) analysis on the molecular structure of mesitylene, Spectrochimica Acta Part A: Molecular and Biomolecular Spectroscopy, 116 (2013) 622-634.
[65] R.G. Pearson, Absolute electronegativity and hardness correlated with molecular orbital theory, Proceedings of the National Academy of Sciences, 83 (1986) 8440-8441.
[66] R.G. Pearson, The electronic chemical potential and chemical hardness, Journal of Molecular Structure: THEOCHEM, 255 (1992) 261-270.
[67] W. Yang, W.J. Mortier, The use of global and local molecular parameters for the analysis of the gas-phase basicity of amines, Journal of the American Chemical Society, 108 (1986) 5708-5711.